Serine and glycine are essential for human muscle progenitor cell population expansion

Brandon J. Gheller[1], Jamie E. Blum[1], Erica L. Bender[1], Mary E. Gheller[1], Esther W. Lim[2], Michal K. Handzlik[2], Patrick J. Stover[3], Martha S. Field[1], Benjamin D. Cosgrove[4], Christian M. Metallo[2], and Anna E. Thalacker-Mercer*[1]

[1]Division of Nutritional Sciences, Cornell University, Ithaca, NY, 14853, USA

[2]Department of Bioengineering, University of California San Diego, La Jolla, CA, 92093, USA

[3]College of Agriculture and Life Sciences, Texas A&M University, College Station, TX, 77843, USA

[4]Meining School of Biomedical Engineering, Cornell University, NY, 14853, USA

*Correspondence: aet74@cornell.edu

Summary

Skeletal muscle regeneration is reliant on a population of muscle specific adult stem cells (muscle progenitor cells; MPCs). During regeneration, the MPC population undergoes a transient and rapid period of population expansion, which is necessary to repair damaged myofibers and restore muscle homeostasis. Much research has focused on the age-related accumulation of negative regulators of regeneration, while the age-related decline of nutrient and metabolic determinants of the regenerative process needs examination. We hypothesized that older individuals, a population that is at risk for protein malnutrition, have diminished availability of amino acids that are necessary for MPC function. Here, we identified that levels of the non-essential amino acid serine are reduced in the skeletal muscle of healthy, older individuals. Furthermore, using stable-isotope tracing studies, we demonstrate that primary, human MPCs (*h*MPCs) exhibit a limited capacity for *de novo* biosynthesis of serine and the closely related amino acid glycine. We identified that serine and glycine are essential for *h*MPC proliferation and, therefore, population expansion. Serine and glycine were necessary to support synthesis of the intracellular antioxidant glutathione, and restriction of serine and glycine was sensed in an EIF2α-dependent manner resulting in cell cycle arrest in G0/G1. In conclusion, we elucidate that, despite an absolute requirement of serine/glycine for *h*MPC proliferation, availability of serine in the skeletal muscle microenvironment is limited to the *h*MPCs of healthy older adults and is a likely underlying mechanism for impaired skeletal muscle regeneration with advancing age.

Keywords

"Satellite cell", "Muscle stem cell," "Metabolism, "Aging," "Serine," "Glycine," "Skeletal muscle"

47 **Graphical Abstract**

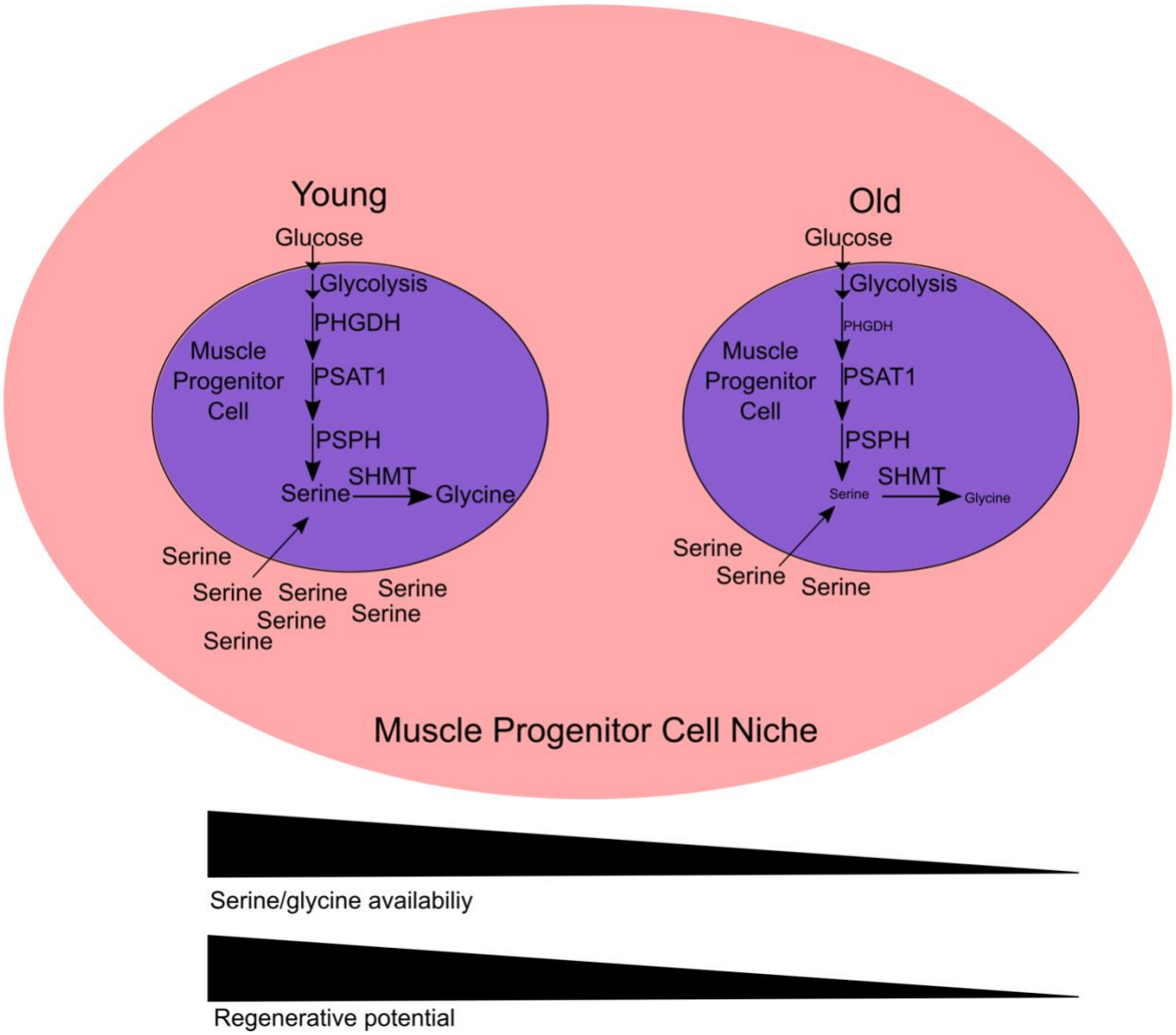

48

49

50

51

52

53

54

55

Introduction

Skeletal muscle regeneration is reliant on a population of muscle specific adult stem/progenitor cells (MPCs) identified by the canonical transcription factor PAX7 (Seale et al., 2000). MPCs reside in a quiescent state, are activated after injury, and undergo a transient and rapid population expansion to provide an adequate number of cells to donate nuclei to damaged myofibers or to create nascent myofibers thereby restoring homeostasis. The muscle regeneration process markedly declines with age due to a myriad of MPC-intrinsic and -extrinsic factors that remain to be fully elucidated (Blau et al., 2015). Parabiosis experiments provide evidence that there are alterations in circulating factors and, ultimately the MPC microenvironment that occurs in aged animals which negatively affects muscle regeneration (Conboy et al., 2005). For example, when the circulation of a young and an aged mouse are joined, muscle regeneration after injury is improved in old mice compared to when the circulation of two old mice are joined (Conboy et al., 2005). Thus, restoration of the MPC microenvironment, to match that of young animals, is a potential avenue for improving skeletal muscle regeneration (Conboy et al., 2005). Follow-up to these landmark studies have largely focused on mechanisms downstream of ligand-based signaling pathways such as the Notch (Conboy et al., 2003) and Wnt (Brack et al., 2007) pathways as well as transforming growth factor beta pathways (Egerman et al., 2015; Sinha et al., 2014). Relatively little attention has focused on nutrient needs and availability to support MPC expansion. Intracellular amino acid availability has been shown to be affected by age in both a cell-intrinsic (e.g., alterations in metabolism) and -extrinsic (e.g., availability in circulation) manner (Dunn et al., 2014; Menni et al., 2013). For example, while gastrointestinal absorption of amino acids after feeding does not appear to be impaired with age (Katsanos et al., 2006; Mitchell et al., 2015), the profile of circulating amino acids is altered by age with lower

levels of serine, alanine, proline, tyrosine, and methionine observed in older individuals (Houtkooper et al., 2011). The importance of amino acid availability to regenerative processes is highlighted by the observation that amino acids are the primary contributors to cell mass during proliferation (Hosios et al., 2016).

It has been previously documented that rapid changes in MPC metabolism occur after activation (Rodgers et al., 2014), likely to support metabolic demands associated with cell division (Hosios et al., 2016). These dynamic, metabolic changes in MPCs are likely accompanied by changes in exogenous nutrient requirements, particularly those traditionally considered non-essential, as demonstrated in other proliferative cell types (Ma et al., 2017). Elucidating the metabolic requirements of MPC proliferation is essential for optimizing muscle regeneration after injury, particularly in populations with impaired regeneration.

We aimed to determine if an age-related decline in amino acid availability exists in the human MPC (*h*MPC) microenvironment and to determine the impact of this amino acid decline on MPC activity if it exists. In this study we identify that serine is the only amino acid that declines in *h*MPC microenvironment with advancing age, and *h*MPCs possess a limited capacity for *de novo* biosynthesis of serine and the closely related amino acid, glycine. Without exogenous serine/glycine, *h*MPCs halt proliferation and arrest in a G0/G1 state. We attribute the requirement for exogenous serine/glycine in part to the need for glutathione synthesis and determined that the G0/G1 cell cycle arrest that occurs in response to serine/glycine restriction occurs in an EIF2α-dependent manner.

Results

Serine availability and metabolism is dysregulated in aged skeletal muscle

Analysis of human skeletal muscle biopsy tissue identified serine as the only measured amino acid that was reduced in the skeletal muscle of older adults compared to younger adults (**Figure 1A**). Further, chronological age and skeletal muscle serine levels were negatively correlated (**Figure 1B**). This finding is supported by a previous cross-sectional analysis of plasma from healthy, younger and older individuals which demonstrated that serine levels are reduced in older humans (Kouchiwa et al., 2012). Others have demonstrated that in frail older adults, skeletal muscle concentrations of serine and also glycine are reduced (Fazelzadeh et al., 2016). Coupled with lower circulating levels, decreased skeletal muscle serine levels suggest that after injury and myofiber disruption the *h*MPC microenvironment of aged individuals has less serine and potentially less glycine available.

To determine what limits serine levels in older skeletal muscle, we measured the gene expression of the serine transporter *SLC1A5* in skeletal muscle tissue homogenates from younger and older adults and found no age-related differences in expression (**Figure 1C**). We next measured gene expression of the serine synthesis enzymes, *PHGDH*, *PSAT1*, and *PSPH* in skeletal muscle tissue homogenates. *PSAT1* was the only gene that was differentially expressed in skeletal muscle with age (1.4-fold greater in older vs. younger, **Figure 1D**). Thus, it is unclear whether impaired uptake or biosynthesis limits serine levels in old muscle tissue.

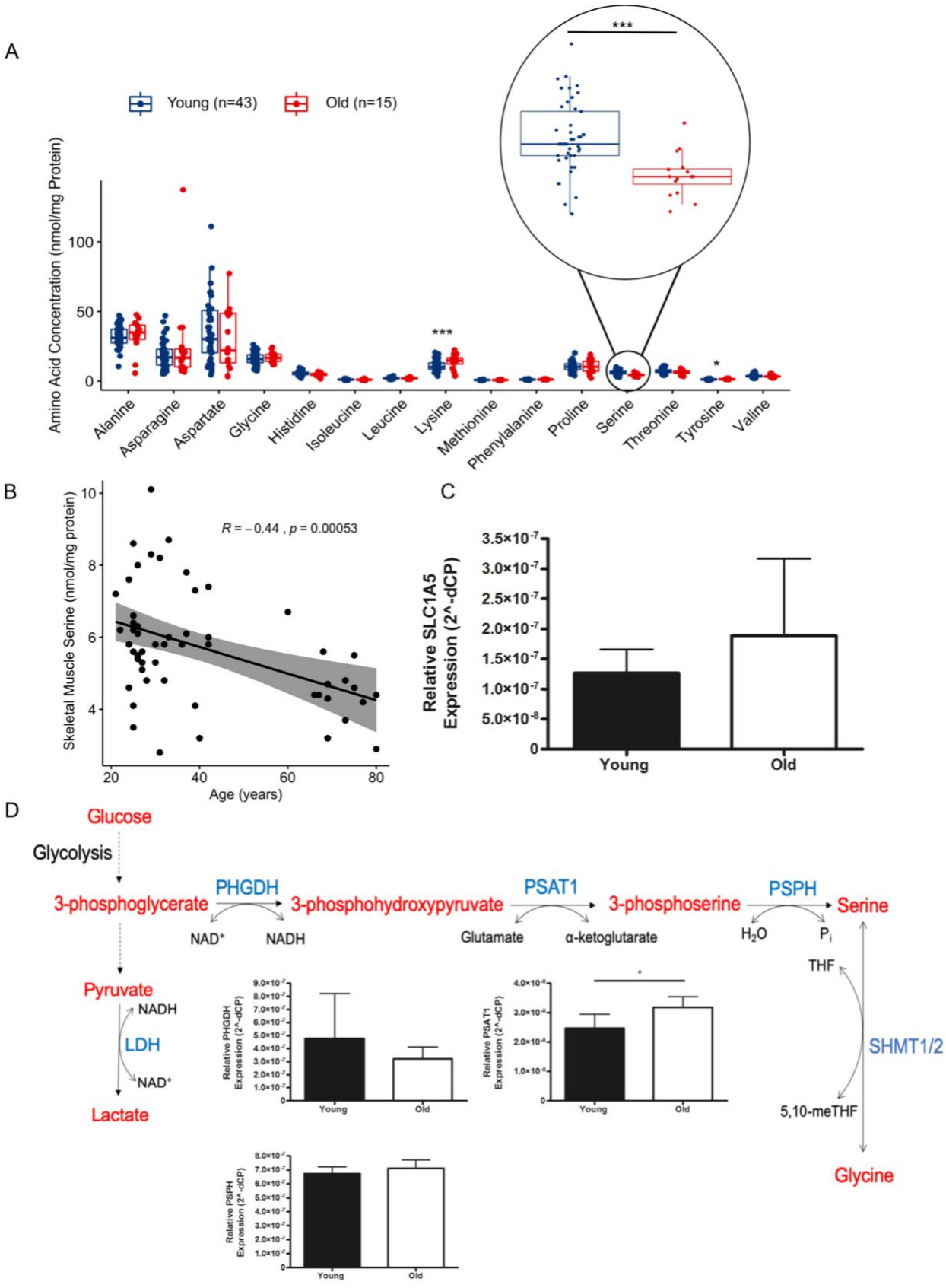

121

Figure 1. Serine availability and metabolism are dysregulated in aged skeletal muscle and *h*MPCs.

A) Analysis of amino acid levels in skeletal muscle biopsy tissue from younger (20-45y, n=43) and older (60-80y, n=15) donors identify serine as the only amino acid that decreases with age ($P<0.001$). The normalcy of the distribution of each amino acid was assessed by the Shapiro-Wilk test. If data were determined to be normally distributed, they were compared via an unpaired t-test otherwise they were compared Mann-Whitney U-test.

B) Skeletal muscle serine levels are negatively correlated with age (n=58, r=-.44, $P<0.0001$) based on a Pearson correlation.

C) Gene expression of the serine transporter SLC1A5 ($P>0.05$) between skeletal muscle tissue from younger (n=11) and older donors (n=10). Data expressed as mean ± SD.

D) A schematic of the serine/glycine biosynthesis pathway. Intermediary metabolites in red. Key enzymes in blue. PHGDH, phosphoglycerate dehydrogenase; PSAT1, phosphoserine amino transferase 1; PSPH, phosphoserine phosphatase; SHMT 1/2, serine hydroxy methyltransferase1/2; LDH, lactate dehydrogenase. Gene expression of PHGDH ($P>0.05$), PSAT1 ($P<0.05$), and PSPH ($P>0.05$) between skeletal muscle tissue from younger (n=11) and older donors (n=10). Data expressed as mean ± SD.
*$P<0.05$.

Serine and glycine are required for hMPC population expansion

Because skeletal muscle serine levels and the regenerative potential of *h*MPCs decline with advancing age, and because serine has previously been shown to be the third most consumed metabolite by proliferating mammalian cells (Hosios et al., 2016) we evaluated whether serine and/or glycine impact *h*MPC population expansion. Serine and glycine were considered alone or in combination due to their interconversion through one enzymatic step via the serine hydroxymethyltransferase (SHMT, **Figure 1D**). When *h*MPCs were cultured without serine and glycine, they did not undergo population expansion (**Figure 2A**). The addition of serine (**Figure 2B**) and glycine (**Figure 2C**) individually or in combination (**Figure 2A**) increased *h*MPC population expansion in a dose-dependent manner. At high doses, glycine alone was more effective at increasing *h*MPC population expansion than serine (**Figure 2D**). This is dissimilar to what is observed in other cell types in which serine and not glycine is required for population expansion (Labuschagne et al., 2014; Ma et al., 2017). We verified that serine/glycine restriction in the media reduced intracellular serine and glycine levels (**Figure 2E**).

To determine the physiological relevance of the serine and glycine concentrations used *in vitro*, we measured plasma serine and glycine concentrations from humans under fasting, resting conditions. The levels of plasma serine were between 76 and 212 µmol/L and plasma glycine were between 178 and 632 µmol/L (**Figure 2F**). However, the levels of these amino acids in circulation are frequently elevated above basal values in the non-fasted state (Gannon et al., 2002; Garofalo et al., 2011) Further, it is likely, that the localized, skeletal muscle availability is also a contributing factor. The physiological relevance of the concentrations used for cell culture experiments are also supported by an analysis by Bergström *et al*. demonstrating that in younger

167 adults, skeletal muscle concentrations of serine and glycine are ~980 µmol/L and ~1330 µmol/L,

168 respectively (Bergström et al., 2017).

169

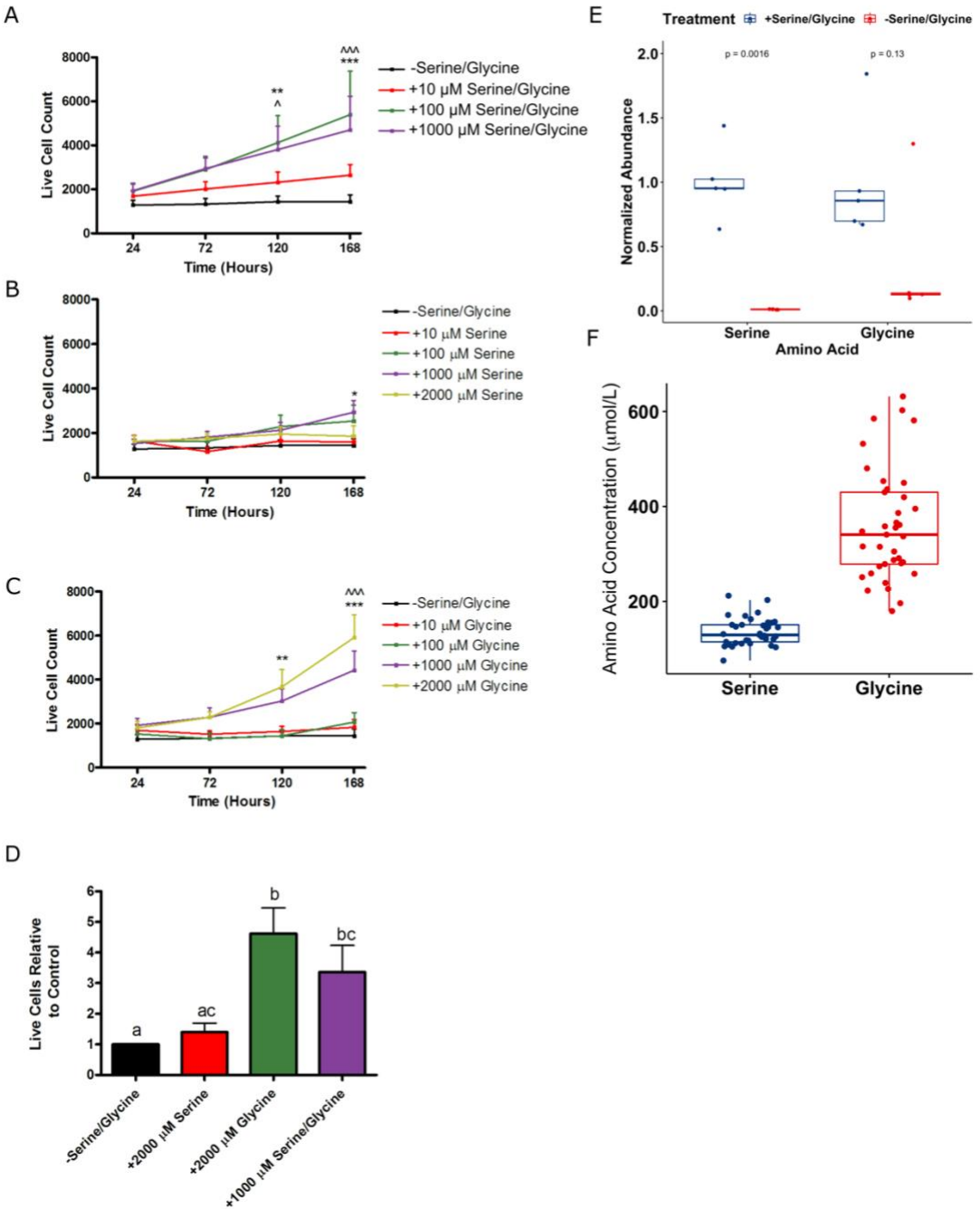

170

Figure 2. Serine and glycine are essential for *h*MPC population expansion.

Live cell count was determined by co-staining cells with Hoescsht 33342 (to identify all cells) and propidium iodide (to identify dead cells) after *h*MPCs were cultured in media lacking serine/glycine or increasing concentrations of

A) serine/glycine (**indicates significant difference between 100 µM vs. -serine/glycine, P<0.01, ***indicates significant difference between 100 µM vs. -serine/glycine, P<0.001, ^indicates significant difference between 1000 µM vs. -serine/glycine, P<0.05, ^^^indicates significant difference between 1000 µM vs. -serine/glycine, P<0.001),

B) serine alone (*indicates significant difference between 1000µM vs. -serine/glycine, P<0.05), or

C) glycine alone (**indicates significant difference between 2000 µM vs. -serine/glycine, P<0.01, ***indicates significant difference between 2000 µM vs. -serine/glycine, P<0.001, ^^^indicates significant difference between 1000 µM vs. -serine/glycine, P<0.001) Data are expressed as mean ± SD.

D) The relative number of live cells after seven days of culture with the indicated concentrations of serine, glycine, or serine and glycine. Different letters are significantly different from each other.

E) Levels of serine and glycine after 7 days of culture in serine/glycine restricted media as determined by GC-MS.

F) Levels of serine and glycine in the plasma of fasted, young humans (n=37) based on GC-MS measurements.

Serine/glycine restriction causes cell cycle arrest

We next sought to understand what drives differences in *h*MPC population expansion when *h*MPCs are cultured with and without serine/glycine. We observed that differences in population expansion, during serine/glycine restriction, could not be explained by cell death (**Figure 3A**). Using DNA staining and analysis via flow cytometry, we observed a greater number of cells in the early phases of the cell cycle with serine/glycine restriction (**Figure 3B**). This finding was supported by reduced incorporation of BrdU into DNA after a 24-hour pulse (**Figure 3C**) and an accumulation of CYCLIN D1 protein in *h*MPCs cultured in serine/glycine restricted media (**Figure 3D**). Because *h*MPC differentiation is modeled *in vitro* by serum restriction (Pavlidou et al., 2017), we measured the *h*MPC specific, mid-to late-differentiation marker MYOGENIN, which was undetectable (**Figure 3E**). Additionally, levels of PAX7 and MYOD were significantly elevated in serine/glycine restricted *h*MPCs (**Figure 3E**). Elevated MYOD levels further supports cell cycle arrest in G1; MYOD protein levels are typically increased in *h*MPCs during G1 of the cell cycle (Kitzmann et al., 1998).

Previously, several proliferative cell types have demonstrated an exogenous requirement for serine/glycine (Labuschagne et al., 2014; Ma et al., 2017). The serine/glycine requirement in these cell types was attributed to DNA synthesis as the proliferative arrest can be rescued by glycine and formate, a one carbon unit integrated into the purine ring structure and necessary for the synthesis of thymidine, or by exogenous nucleotides. In contrast, in *h*MPCs the serine/glycine requirement appears to be derived from glycine (**Figure 2CD**) and is not DNA synthesis based as supplementation with nucleotide precursors did not rescue *h*MPC population expansion (**Figure 3F**).

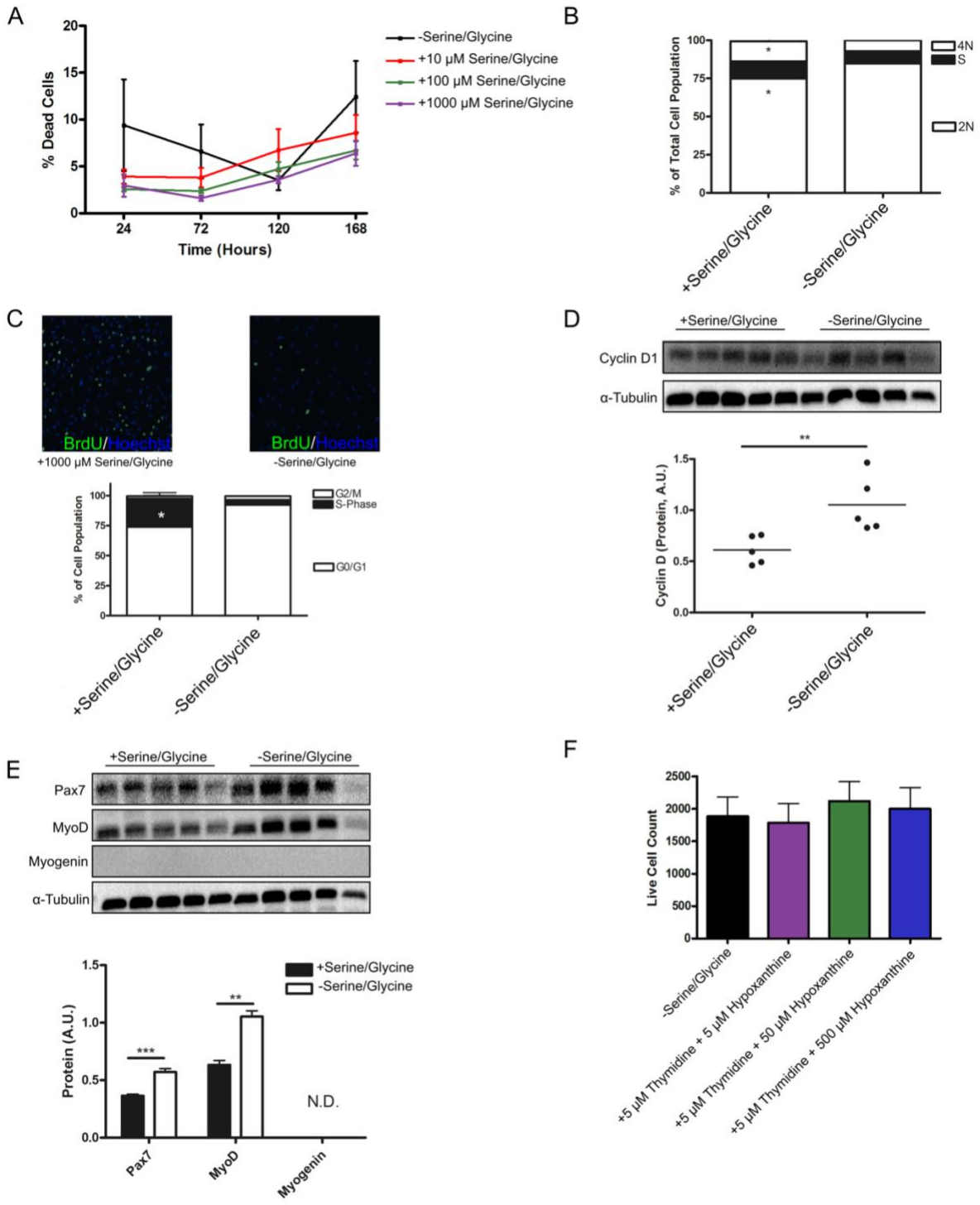

217

218

219

Figure 3. Serine/glycine restriction causes cell cycle arrest in G0/G1 in *h*MPCs.

A) Percentage of dead cells was quantified by dividing all *h*MPCs which stained positive for propidium iodide by all *h*MPCs which stained positive for Hoechst 33342 after 5 days of culture in media with varying concentrations of serine/glycine.

B) Propidium iodide staining and analysis via flow cytometry was used to determine DNA content of *h*MPCs after 5 days of serine/glycine restriction. *P<0.05.

C) BrdU incorporation in after a 24-hour pulse in *h*MPCs undergoing serine/glycine restriction for 5 days. Data are expressed as mean ± SD.

D) Immunoblot for CYCLIN D1 protein normalized to α-TUBULIN for quantification in *h*MPCs that had been serine/glycine restricted for 5 days. **P<0.01.

E) Immunoblot for PAX7, MYOD, and MYOGENIN protein normalized to α-TUBULIN for quantification in *h*MPCs that had been serine/glycine restricted for 5 days. **P<0.01, ***P<0.001. N.D., not detectable. Data are expressed as mean ± SD.

F) Live cell count for *h*MPCs treated with varying concentrations of thymidine and hypoxanthine. Data are expressed as mean ± SD.

All experiments were repeated with *h*MPCs derived from the same 5 donors.

hMPCs exhibit limited capacity for serine/glycine biosynthesis

We hypothesized that *h*MPCs lack the ability for *de novo* serine/glycine biosynthesis, and that this underlies the exogenous requirements when *h*MPCs are cultured *in vitro*. In contrast to this hypothesis, RNA-seq analyses revealed that *h*MPCs drastically upregulate serine/glycine biosynthesis genes in response to serine/glycine restriction (**Figure 4A, Table S1**). We further verified that the enzymes directly implicated in serine/glycine biosynthesis (PHGDH, PSPH, PSAT1, SHMT1, SHMT2) are expressed at the protein level and the serine synthesis proteins, specifically, are upregulated in response to serine/glycine restriction (**Figure 4B**). The serine synthesis pathway branches from glycolysis at 3-phosphoglycerate, using glucose as the initial substrate (**Figure 1D**); however, glucose uptake did not increase after serine/glycine restriction (**Figure 4C**). Further, increasing glucose concentrations in the media did not affect *h*MPC proliferation in the absence of serine/glycine (**Figure 4D**), which suggests a limited capacity for serine/glycine biosynthesis by *h*MPCs. Using stable isotope tracing with $^{13}C_6$ glucose, we determined that *de novo* biosynthesis accounts for no detectable intracellular serine and glycine when serine/glycine are available in the media (**Figure 4E**). During serine/glycine restriction, *de novo* biosynthesis contributes ~25% of serine and ~5% of glycine to the intracellular pools (**Figure 4E**) demonstrating that *h*MPCs have the capacity for serine/glycine biosynthesis under restricted conditions. However, the increase in *de novo* biosynthesis is ineffective to maintain the requirements for population expansion as highlighted by the low levels of relative serine and glycine even when *de novo* biosynthesis is active (**Figure 2E**). Even if *h*MPCs were able to synthesize sufficient serine and glycine to support proliferation, we identified that primary *h*MPCs from older adults have reduced expression of the serine biosynthesis enzyme PHGDH, (**Figure 4F**, n=10) suggesting that *h*MPC-intrinsic *de novo* serine synthesis is likely impaired.

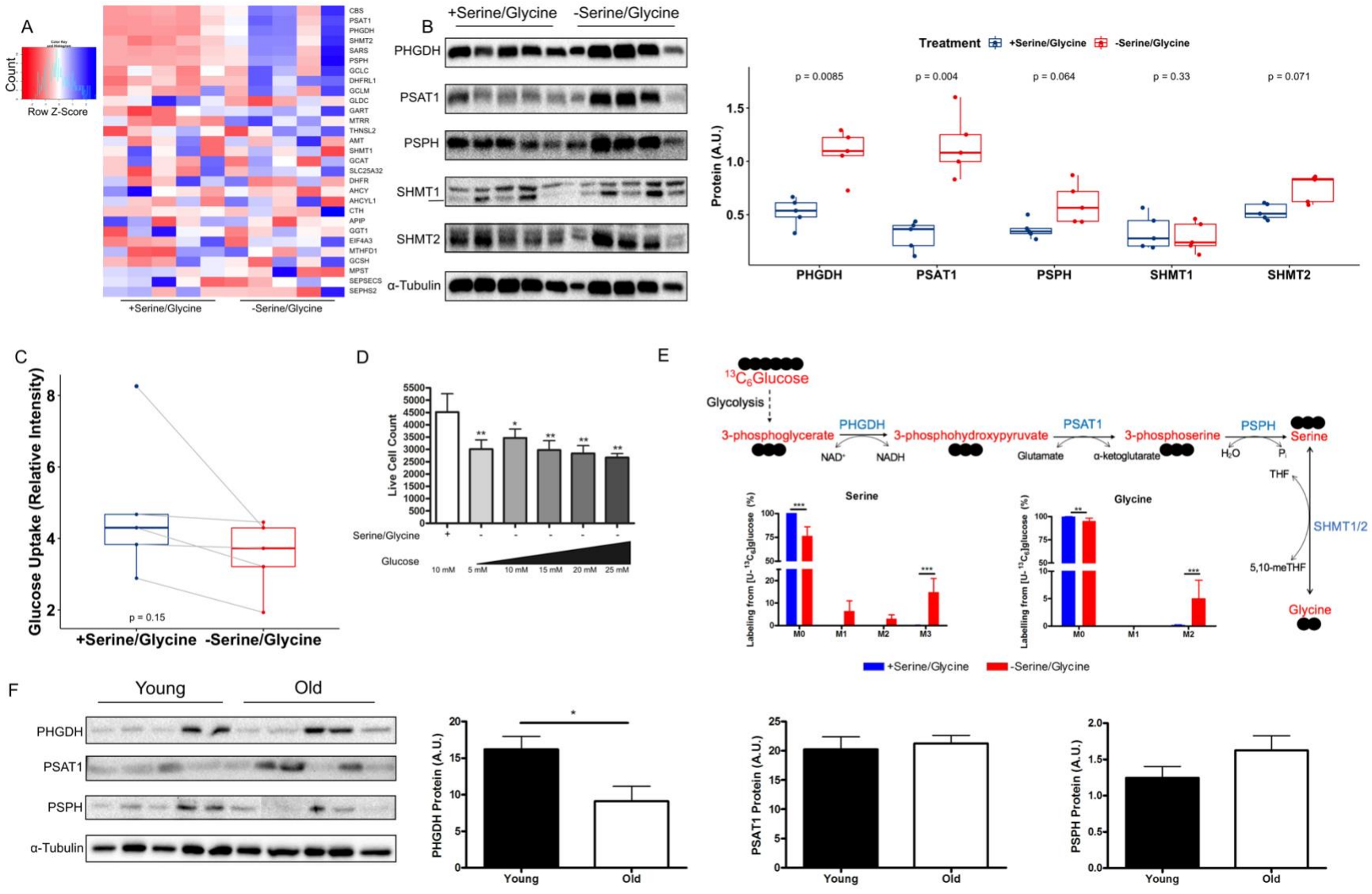
A
Count
Row Z-Score
CBS
PSAT1
PHGDH
SHMT2
SARS
PSPH
GCLC
DHFRL1
GCLM
GLDC
GART
MTRR
THNSL2
AMT
SHMT1
GCAT
SLC25A32
DHFR
AHCY
AHCYL1
CTH
APIP
GGT1
EIF4A3
MTHFD1
GCSH
MPST
SEPSECS
SEPHS2
+Serine/Glycine
-Serine/Glycine
B
+Serine/Glycine
-Serine/Glycine
PHGDH
PSAT1
PSPH
SHMT1
SHMT2
α-Tubulin
Treatment
+Serine/Glycine
-Serine/Glycine
p = 0.0085
p = 0.004
p = 0.064
p = 0.33
p = 0.071
Protein (A.U.)
PHGDH
PSAT1
PSPH
SHMT1
SHMT2
C
Glucose Uptake (Relative Intensity)
p = 0.15
+Serine/Glycine
-Serine/Glycine
D
Live Cell Count
Serine/Glycine
Glucose
10 mM
5 mM
10 mM
15 mM
20 mM
25 mM
E
13C6Glucose
Glycolysis
3-phosphoglycerate
PHGDH
NAD+
NADH
3-phosphohydroxypyruvate
PSAT1
Glutamate
α-ketoglutarate
3-phosphoserine
PSPH
H2O
Pi
Serine
THF
SHMT1/2
5,10-meTHF
Glycine
Serine
Glycine
Labeling from [U-13C6]glucose (%)
M0
M1
M2
M3
+Serine/Glycine
-Serine/Glycine
F
Young
Old
PHGDH
PSAT1
PSPH
α-Tubulin
PHGDH Protein (A.U.)
PSAT1 Protein (A.U.)
PSPH Protein (A.U.)
Young
Old

Figure 4. *h*MPCs exhibit limited capacity for serine/glycine biosynthesis.

A) Heatmap of genes involved in serine, glycine, and one-carbon metabolism based on RNA-sequencing data from *h*MPCs after 5 days of culture in serine/glycine replete (1000 µM) or restricted conditions.

B) Immunoblots for PHGDH, PSAT1, PSPH, SHMT1, and SHMT2 protein normalized to α-TUBULIN for quantification in *h*MPCs that had been serine/glycine restricted for 5 days.

C) Glucose uptake by *h*MPCs after 5 days of culture in serine/glycine replete or restricted conditions.

D) Live cell count of *h*MPCs cultured in serine/glycine replete media or serine/glycine restricted media and varying doses of glucose. *P<0.05, **P<0.01 relative to serine/glycine containing control. Data are expressed as mean ± SD.

E) Percent mass isotopomer distribution of [U-^{13}C]-glucose-derived serine and glycine in *h*MPCs cultured in serine/glycine replete (1000 µM) or restricted media for 5 days followed by 48 hours in similar media but containing [U-^{13}C]-glucose. Data are expressed as mean ± SD.

F) Protein levels of the serine/glycine biosynthesis enzymes PHGDH, PSAT1, and PSPH in *h*MPCs obtained from younger (n=5) and older (n=5) individuals as determined by immunoblotting. *P<0.05. Data expressed as mean ± SD.

All experiments were repeated with *h*MPCs derived from the same 5 donors. P-values are indicated on the appropriate graphs.

290 *Serine/glycine restriction promotes oxidative stress in hMPCs and depletes intracellular*
291 *glutathione*

292 Several genes related to glutathione biosynthesis were upregulated with serine/glycine
293 depletion in the transcriptomic dataset (**Figures 4A, Figure 5A, Table S1**). Because glycine is
294 one of the three amino acids that comprise the tripeptide glutathione, we hypothesized that
295 serine/glycine restriction reduced glutathione levels in *h*MPCs and impaired population
296 expansion. Serine/glycine restriction decreased total glutathione levels by approximately 9-fold
297 in *h*MPCs (**Figure 5B**) and decreased the ratio of GSH:GSSG (**Figure 5C**). As would be
298 expected with lower glutathione levels, the primary intracellular antioxidant, we observed an
299 increase in the levels of reactive oxygen species (ROS, **Figures 5D**). Supplementation with a cell
300 permeable version of glutathione, glutathione ethyl ester (GSHee), modestly increased
301 intracellular glutathione levels (**Figure 5E**) and decreased ROS levels (**Figure 5F**). Despite only
302 a modest effect on intracellular glutathione levels, GSHee did provide a minor rescue to *h*MPC
303 population expansion (**Figure 5G**). Of note, high levels of cell permeable glutathione were toxic
304 (**Figure S1**) and therefore, we were not able to investigate how increasing intracellular levels of
305 glutathione to that observed in serine/glycine replete cells would impact *h*MPC population
306 expansion. We propose that ROS, associated with *h*MPC proliferation, cannot be
307 counterbalanced during serine/glycine restriction due to reduced glutathione synthesis caused by
308 limited serine/glycine synthesis leading to cell cycle arrest.
309

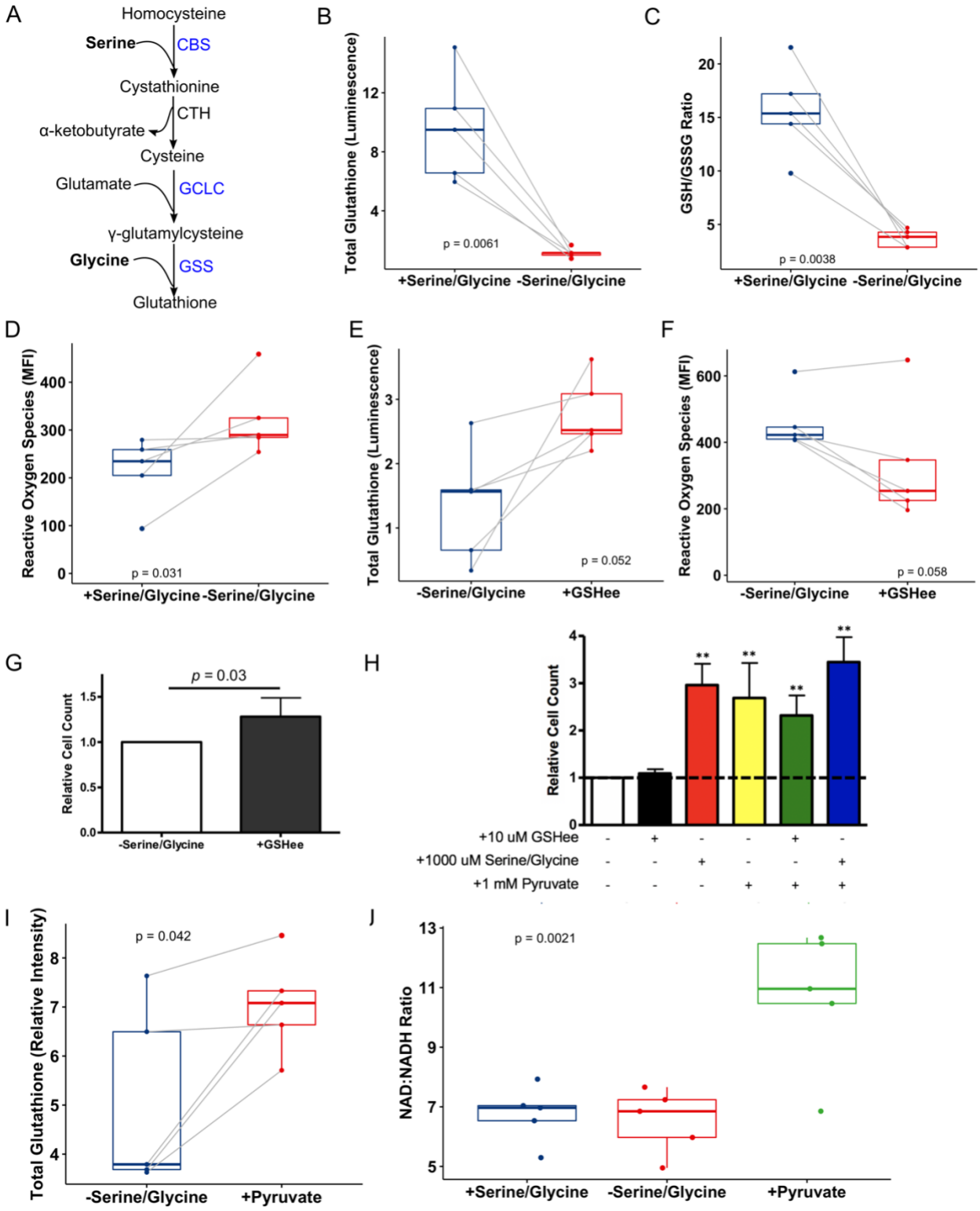

Figure 5. Serine/glycine restriction impairs glutathione synthesis but can be rescued by pyruvate supplementation.

A) The glutathione synthesis pathway with genes upregulated after serine/glycine restriction according to RNA-sequencing in blue. CBS, cystathionine β-synthase; CTH, cystathionine gamma-lyase; GCLC, glutamate-cysteine ligase catalytic subunit; GSS, glutathione synthetase.

B) Total intracellular glutathione levels in *h*MPCs after 5 days in serine/glycine restricted or replete media.

C) Ratio of reduced to oxidized intracellular glutathione levels in *h*MPCs after 5 days in serine/glycine restricted or replete media. GSH, reduced glutathione; GSSG, oxidized glutathione.

D) Reactive oxygen species in *h*MPCs after 5 days in serine/glycine restricted or replete media.

E) Total intracellular glutathione levels in *h*MPCs after 5 days of serine/glycine restriction with or without 10 μM cell permeable glutathione ethyl ester (GSHee).

F) Reactive oxygen species in *h*MPCs after 5 days of serine/glycine restriction with or without 10 μM GSHee.

G) Live cell count after 5 days of serine/glycine restriction with or without GSHee (10 μM).

H) Live cell count after 5 days of the indicated combination and concentration of serine/glycine, GSHee, and pyruvate. **P<0.01

I) Total glutathione levels in *h*MPCs cultured in a serine/glycine restricted media with or without 1 mM pyruvate for 5 days.

J) Ratio of oxidized NAD (NAD^+):reduced NAD (NADH) in *h*MPCs cultured in restricted serine/glycine media or media containing 1000 µM serine/glycine or 1 mM pyruvate.

All experiments were repeated with *h*MPCs derived from the same 5 donors. P-values are indicated on the appropriate graphs.

Pyruvate rescues hMPC proliferation during serine/glycine restriction

Under the assumption that inadequate glycine availability prevents adequate glutathione synthesis and ROS scavenging, we provided pyruvate in the absence of serine/glycine as an alternative antioxidant; we observed a complete rescue of the proliferative defect caused by serine/glycine restriction (**Figure 5H**). Pyruvate also increased total glutathione levels (**Figure 5I**). An additional mechanism by which pyruvate supplementation may have rescued *h*MPC proliferation, during serine/glycine restriction, is by increasing the NAD^+/NADH ratio through the reduction of pyruvate to lactate, which provides the necessary NAD^+ cofactor for serine biosynthesis (i.e., for the conversion of 3-phosphoglycerate to 3-phosphohydroxypyruvate, **Figure 1C**). Supporting this mechanism, pyruvate supplementation, in the absence of exogenous serine/glycine, increased the NAD^+/NADH ratio which has recently been identified as the limiting cofactor for serine biosynthesis (Diehl et al., 2019) (**Figure 5J**).

Serine/glycine restriction induces the integrated stress response in hMPCs

We hypothesized that ATF4 may integrate the sensing of serine/glycine restriction and underlie the transcriptional upregulation of the serine/glycine biosynthetic genes (**Figure 4A**). We noted several ATF4 target genes that were affected by serine/glycine restriction in *h*MPCs (**Figure 6A**). We further verified that protein levels of ATF4 and its upstream regulator, p-eIF2α, are increased after serine/glycine restriction (**Figure 6B**). Phosphorylation of eIF2α is known to coordinate a global decline in protein synthesis. In support of this, in the absence of serine/glycine, we observed an accumulation of most of the free, non-serine/glycine amino acids (**Figure 6C**) and a trend towards reduced protein synthesis (assessed by puromycin incorporation, **Figure 6D**).

379 To directly test whether the p-eIF2α response was responsible for arrest of *h*MPC
380 proliferation, *h*MPCs were cultured with the small molecule, p-eIF2α inhibitor, ISRIB (Sidrauski
381 et al., 2015) (**Figure 6E**). Treatment with ISRIB increased *h*MPC cell number in the absence of
382 serine/glycine (**Figure 6F**). Interestingly, ISRIB treatment, in the presence of serine/glycine,
383 negatively affected cell number (**Figure S2**) suggesting that the benefit of reducing p-eIF2α
384 signaling on *h*MPC proliferation was only effective when aberrant signaling was induced by
385 serine/glycine restriction. Therefore, we propose that serine/glycine restriction reduces the
386 intracellular availability of serine, glycine, and glutathione, which activates the integrated stress
387 response and leads to limited global translation and further to cell cycle arrest (**Figure 6G**).
388 Overall, this process is likely exacerbated in older adults who lose serine availability in the
389 microenvironment.
390

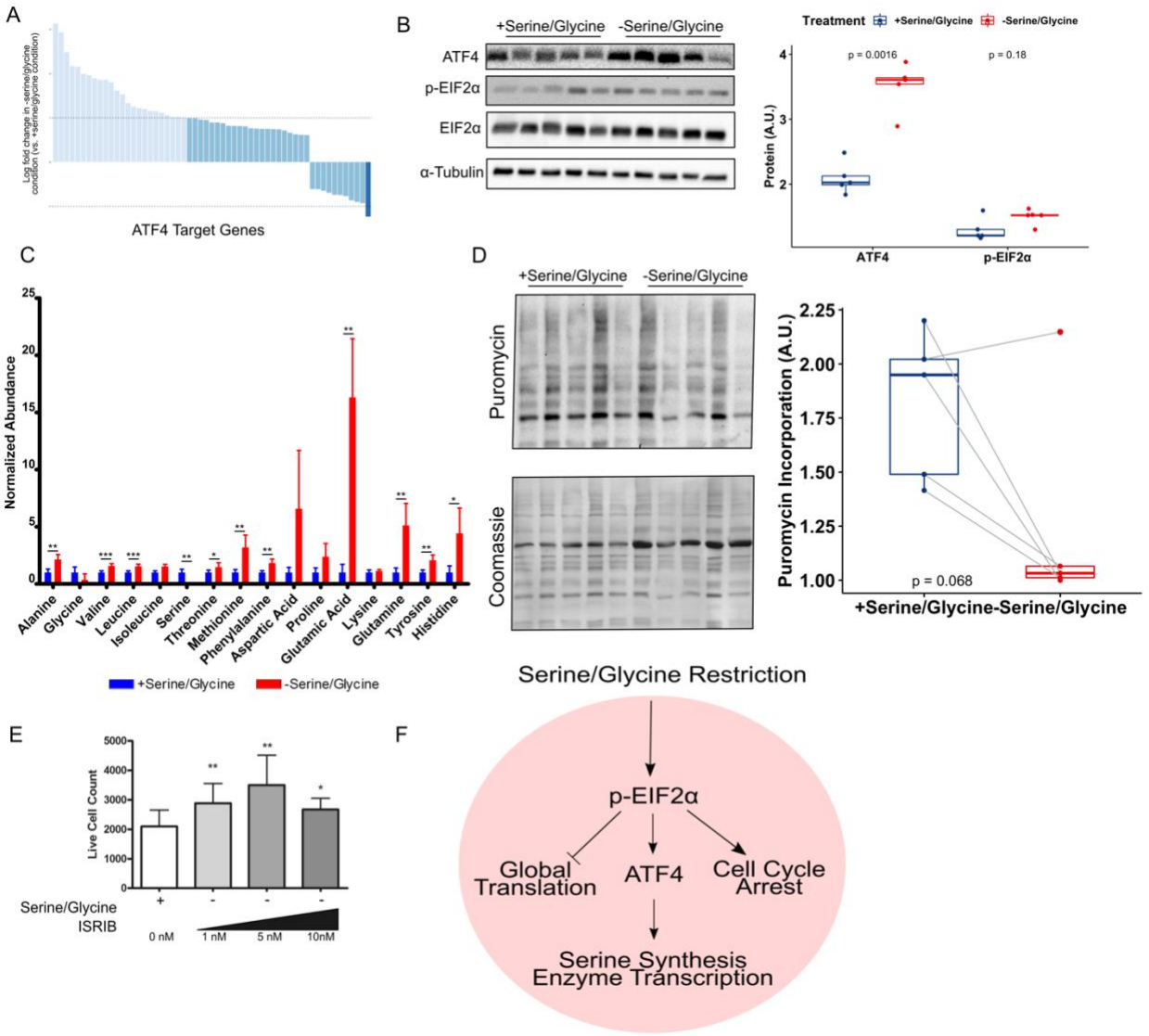

Figure 6. Serine/glycine restriction activates ATF4 in a p-EIFα dependent manner causing *h*MPC proliferation arrest.

A) Expression of known ATF4 targets based on RNA-sequencing of *h*MPCs cultured in serine/glycine restricted media or serine/glycine replete media for 5 days. Average log fold change of transcripts in serine/glycine restricted samples vs. serine/glycine replete samples. Dark blue indicates fold change < -1 and light blue indicates fold change > 1.

B) Left, protein levels of ATF4, p-eIF2α, and total eIF2α determined by immunoblotting *h*MPCs cultured in serine/glycine replete or restricted media. All proteins were normalized to α-TUBULIN expression. Right, quantification of protein expression.

C) Intracellular amino acid abundance, normalized to total ion count, in *h*MPCs cultured in serine/glycine replete or restricted media for 5 days.

D) Left, immunoblot analysis for puromycin incorporation of *h*MPCs cultured in serine/glycine replete or restricted media for 5 days normalized to Coomassie staining. Right, quantification of puromycin incorporation.

E) Protein levels of p-eIF2α and total eIF2α determined by immunoblotting in *h*MPCs cultured in serine/glycine restricted media with and without 5 nM ISRIB. All proteins were normalized to α-TUBULIN expression. Right, quantification of protein expression.

F) Live cell count after 5 days of serine/glycine restriction with or without varying doses of ISRIB.

G) Generalized model of how serine/glycine restriction affects EIF2α and ATF4 to reduce global protein synthesis and cause cell cycle arrest.

All experiments were repeated with *h*MPCs derived from the same 5 donors. P-values are indicated on the appropriate graphs.

Discussion

Here, we report that aging reduces levels of serine in the *h*MPC microenvironment and that *h*MPCs are limited in their capacity for serine/glycine biosynthesis. The negative correlation between skeletal muscle levels of serine and age are in line with previous analyses comparing serum of younger and older individuals (Dunn et al., 2014; Menni et al., 2013). While glycine has not consistently been noted as reduced in the circulation of older adults, it has been shown to be reduced in the red blood cells of older adults and these reduced levels can be corrected by dietary supplementation (Sekhar et al., 2011). In support of a dysregulation of serine synthesis with age, we identified changes in expression of the serine synthesis enzymes with age in whole skeletal muscle tissue and in isolated *h*MPCs. Others have previously identified that the expression of metabolic enzymes and nutrient transporters can decline with age, however, the underlying reason for this remains elusive (Kawase et al., 2015). While our data are supportive of a decrease of serine levels in human skeletal muscle with age, potentially due to reduced biosynthesis, a direct measurement is necessary to definitively answer this question. Therefore, it is likely that reduced availability of serine/glycine to *h*MPCs is due to a combination of reduced *de novo* synthesis and dietary changes or metabolism with age.

The importance of decreased serine/glycine availability to *h*MPCs with age is highlighted by our identification of an absolute requirement for the non-essential amino acids, serine and glycine, for *h*MPC proliferation. A previous report, in rat MPCs, demonstrated that serine and glycine are required for proliferation likely due to a limited capacity for *de novo* serine synthesis (Dufresne et al., 1976). A more recent report found that C2C12 cells, an immortalized murine cell line mimicking MPCs, could proliferate in the presence of serine and absence of glycine but that proliferation was enhanced with the addition of glycine (Sun et al., 2016). It is possible that

445 glycine in the C2C12 cell model is synthesized from serine to maintain necessary glycine for
446 cellular processes, however, isotope tracing was not conducted to test this theory. The work
447 presented here builds upon these previous findings by extending them into a primary, human
448 model and elucidating the mechanism for the *h*MPC serine/glycine requirement.

449 The skeletal muscle of older individuals has a diminished ability to regenerate after injury
450 due to a decline in the function of MPCs. It has been demonstrated that repeated muscle injury in
451 aged mice depletes the number of self-renewing MPCs and consequently skeletal muscle
452 regeneration (Sousa-Victor et al., 2014). *h*MPCs isolated from older (vs. younger) donors exhibit
453 diminished antioxidant capacity (Fulle et al., 2005) and *h*MPCs that are undergoing replicative
454 senescence in culture, to model aging, exhibit increased ROS levels (Minet and Gaster, 2012).
455 Together, this suggests that *h*MPCs from older individuals may have diminished skeletal muscle
456 regeneration because of an inability to buffer the ROS produced as a natural consequence of
457 proliferation (L'Honoré et al., 2018). Serine/glycine are required for glutathione synthesis to
458 maintain physiological levels of ROS (L'Honoré et al., 2018) during proliferation as
459 demonstrated by our experiments in which supplementation of cell-permeable glutathione,
460 increased cell number in a modest but repeatable manner. Therefore, a decline in serine
461 availability in the *h*MPC microenvironment, coupled with a decline in the *h*MPC-intrinsic
462 capacity for *de novo* serine synthesis, may prevent adequate glutathione synthesis to buffer
463 proliferation associated increases in intracellular ROS and lead to a reduction in the MPC pool in
464 older individuals. Evidence exists that dietary intervention may be able to help maintain
465 glutathione levels with advancing age. For example, a persistent metabolic phenotype associated
466 with aging skeletal muscle is increased ROS due to impaired glutathione synthesis and this
467 phenotype can be corrected with dietary supplementation of the glutathione precursors glycine

and cysteine (Sekhar et al., 2011). Future studies should examine the effect of dietary supplementation on glutathione production by aged MPCs.

There is a growing body of literature demonstrating that dietary glycine supplementation protects muscle mass and function during a number of disease states including cancer cachexia (Ham et al., 2014), muscle dystrophy (Ham et al., 2019), sepsis (Ham et al., 2016), and reduced calorie intake (Caldow et al., 2016). To date the beneficial effects of glycine supplementation on skeletal muscle in the disease state has been attributed to glycine's systemic anti-inflammatory effects, its contribution to balancing ROS signaling in whole skeletal muscle tissue, and its ability to restore skeletal muscle's anabolic response to leucine (Koopman et al., 2017). However, muscle dystrophy, specifically, is characterized by chronic MPC proliferation (Carnwath and Shotton, 1987) and genetic perturbations in MPCs have been shown to improve mouse models of muscle dystrophy by supporting maintenance of the MPC population (Gallot et al., 2018). Therefore, while much research has focused on understanding the role of dietary glycine supplementation on mature skeletal muscle as a mechanism for attenuating disease related skeletal muscle loss our data suggest that such dietary supplementation may also contribute to skeletal muscle maintenance by supporting MPC proliferation.

We demonstrate that inadequate intracellular serine/glycine and/or subsequent alterations in intracellular metabolism can be sensed in a p-eIF2α dependent manner resulting in halted protein translation and cell cycle arrest. eIF2α is a stress-sensing kinase that can integrate inputs from a number of signals to elicit the integrated stress response that directs ATF4 to upregulate genes associated with metabolism and nutrient uptake while limiting the expression of genes that are non-essential for immediate survival (Harding et al., 2003). The serine/glycine biosynthesis enzymes have been identified as ATF4 targets (DeNicola et al., 2015), highlighting the

491 importance of this pathway in mediating cell survival under stress conditions. It is unknown
492 whether the stress signal, which elicited the ATF4 response in *h*MPCs, was the low levels of
493 serine/glycine themselves, the buildup of ROS caused by reduced glutathione levels, or through
494 another mechanism. eIF2α is also a primary regulator of protein translation (Holcik and
495 Sonenberg, 2005) and we demonstrated, in *h*MPCs, that serine/glycine restriction results in a
496 reduction of protein translation and an accumulation of free amino acids. Inhibition of protein
497 translation via a number of different approaches arrests cells in the G1 phase of the cell cycle
498 (Polymenis and Aramayo, 2015). Similarly, phosphorylation of eIF2α has been previously
499 shown to be associated with fibroblast arrest in the G1 phase of the cell cycle; however, in
500 opposition to our results, arrest in G1 by fibroblasts was associated with a decrease in cyclin D1
501 translation (Hamanaka et al., 2005). In quiescent MPCs eIF2α is maintained in a phosphorylated
502 state and ATF4 levels are abundant (Zismanov et al., 2016). When MPCs transition from
503 activation to proliferation p-eIF2α as well as ATF4 levels decline (Zismanov et al., 2016).
504 Furthermore, a point mutation in MPCs that prevents the phosphorylation of eIF2α forces MPCs
505 to break quiescence, a state of cell cycle arrest, and initiate proliferation (Zismanov et al., 2016).
506 These results are similar to those found in this report when the cell cycle arrest initiated by
507 serine/glycine restriction was overcome by treatment with ISRIB, an inhibitor of p-eIF2α.

508 For the first time, we identified that *h*MPCs possess the capacity for *de novo*
509 serine/glycine biosynthesis. Intriguingly, we note that serine/glycine biosynthesis only occurs
510 when *h*MPCs are challenged with exogenous serine/glycine restriction. Furthermore, when
511 serine/glycine synthesis does occur it is ineffective at restoring intracellular levels of
512 serine/glycine to a degree necessary to support proliferation. The limited ability of *h*MPCs to
513 produce adequate serine/glycine is at least partially attributable to a lack of NAD^+ to facilitate the

conversion of 3-phosphoglycerate to 3-phosphohydroxypyruvate and eventually serine rather than a lack of glucose to form 3-phosphoglycerate. This assertion is supported by the fact that addition of pyruvate which is converted to lactate via lactate dehydrogenase, a reaction which also oxidizes NADH to NAD^+, increased the ratio of NAD^+/NADH and rescued *h*MPC proliferation. Additionally, serine/glycine restriction did not increase glucose uptake nor did increasing levels of available glucose influence *h*MPC proliferation, suggesting that the limitation of serine synthesis was not driven by glycolytic substrate availability. We did note that serine/glycine restriction did not increase cell death and therefore it may be that serine/glycine biosynthesis is upregulated in serine/glycine deplete conditions to support cell survival.

In conclusion, we have outlined a novel requirement for exogenous serine/glycine to support *h*MPC proliferation. Furthermore, we have identified that the reduced availability of extracellular and intracellular serine/glycine in aging may contribute to the decline in *h*MPC-based skeletal muscle regeneration that occurs with aging.

Methods

Participants

Younger (21-40 years) and older adults (65-80 years) were recruited from the Tompkins County, New York area. Participants were excluded if they had a history of negative or allergic reactions to local anesthetic, used immunosuppressive medications, were prescribed to anti-coagulation therapy, were pregnant, had a musculoskeletal disorder, suffered from alcoholism (>11 drinks per week for women and >14 drinks per week for men) or other drug addictions, or were acutely ill at the time of participation (Gheller et al., 2019a; Riddle et al., 2018a). The Cornell University, Institutional Review Board approved the protocol and all subjects gave written informed consent in accordance with the Declaration of Helsinki.

Human skeletal muscle biopsies

Skeletal muscle tissue was obtained from the vastus lateralis muscle of humans using the percutaneous biopsy technique. Visible connective or adipose tissues were removed at the time of biopsy. For tissue homogenate experiments the biopsy sample was measured for wet weight and then snap-frozen in liquid nitrogen and stored at -80$_{o}$C. For cell culture experiments a 60-100 mg portion of the tissue was stored in Hibernate®-A medium (Invitrogen) at 4$_{o}$C until tissue disassociation was performed (within 48 hours).

Amino acid analysis of human skeletal muscle tissue

Frozen tissue samples (20-30 mg) were homogenized for 2 min using ceramic beads (Precellys 2 mL Hard Tissue Homogenizing Ceramic Beads Kit, Bertin Instruments, US) in 500 µL -20°C methanol, 400 µL ice-cold saline, and 100 µL ice-cold H_2O containing amino acid isotope labelled internal standards (Cambridge Isotope Laboratories, #MSK-A2-1.2). An aliquot of tissue homogenate (50 µL) was dried under air and resuspended in RIPA buffer for protein

quantification using bicinchoninic acid assay (BCA, BCA Protein Assay, Lambda, Biotech Inc., US). 1 mL of chloroform was added to the remaining homogenate and the samples were vortexed for 5 min followed by centrifugation at 4°C for 5 min at 15 000 g. The organic phase was collected and the remaining polar phase was re-extracted with 1 mL of chloroform. An aliquot of the polar phase was collected, vacuum-dried at 4°C, and subsequently derivatized with 2% (w/v) methoxyamine hydrochloride (Thermo Scientific) in pyridine for 60 min following by 30 min sialyation N-tertbutyldimethylsilyl-N-methyltrifluoroacetamide (MTBSTFA) with 1% tert-butyldimethylchlorosilane (tBDMS) (Regis Technologies) at 37°C. Polar derivatives were analyzed by gas chromatography (GC)-mass spectrometry (MS) using a DB-35MS column (30m x 0.25 mm i.d. x 0.25 µm, Agilent J&W Scientific) installed in an Agilent 7890A GC interfaced with an Agilent 5975C MS as previously described (Wallace et al., 2018).

Amino acid analysis of human plasma

3 µL of human plasma were spiked with 3 µL amino acid isotope labelled internal standards (Cambridge Isotope Laboratories, #MSK-A2-1.2) and extracted with 250 µL –20 °C methanol for 10 min and centrifuged at 4°C for 10 min at 15 000 g. 200 µL of supernatant was collected, vacuum-dried at 4°C, and derivatized with MTBSTFA and tBDMS as described for muscle polar analysis.

Primary hMPC culture

Primary *h*MPC cultures were obtained as previously described (Riddle, Bender and A. E. Thalacker-Mercer, 2018; Riddle, Bender and A. Thalacker-Mercer, 2018; Gheller, J. Blum, *et al.*, 2019). Briefly, skeletal muscle tissue, stored in Hibernate®-A medium (Gibco), was minced and washed via gravity with Dulbecco's PBS (Gibco) and then digested using mechanical and enzymatic digestion in low glucose Dulbecco's Modified Eagle Medium (Gibco). This solution

583 was passed through a 70 μm cell strainer into 5 mL of a growth media comprised of Ham's F12
584 (Gibco), 20% FBS, 1% penicillin/streptomycin (Corning), and 5 ng/mL recombinant human
585 basic fibroblast growth factor (bFGF, Promega) then centrifuged. The pelleted cells were
586 resuspended in growth media containing 10% DMSO and cryopreserved at -80$_o$C until isolation
587 via flow cytometry. Primary *h*MPCs were sorted using fluorescence activated cell sorting with
588 fluorescently-conjugated antibodies to cell surface antigens specific to *h*MPCs [CD56 (NCAM,
589 BD Pharmingen) and CD29 (β1-integrin, BioLegend)] and a viability stain (7-
590 Aminoactinomycin D, eBioscience) (Xu et al., 2015). Passage six *h*MPCs were used for all
591 experiments and were cultured in a 5% CO_2 atmosphere at 37°C on collagen coated plates (Type
592 I, Rat Tail, Corning). For cell culture experiments, donor cells from females were used
593 exclusively due to availability of adequate sample.

594 *h*MPCs were initially seeded in the growth medium described above before being
595 switched to treatment medium 24 hours later. For all experiments a specially formulated DMEM
596 devoid of serine, glycine, methionine, choline, pyridoxine, glucose, folate, nucleotides, and
597 nucleosides that was supplemented with dialyzed and charcoal treated FBS (10%), 200 μM
598 methionine, 4 mg/L pyridoxine, 5 ng/mL bFGF, 25 nM (6S) 5-formylTHF, penicillin-
599 streptomycin (1%), 10 mmol/L glucose, 4 mM Glutamax (Gibco), as well as L-serine and
600 glycine in varying concentrations. Unless otherwise noted, all assays were performed after 5
601 days in the treatment medium specified as this was the time point when differences in cell
602 number between cells grown in serine/glycine restricted and replete media were initially
603 identified. In all experiments cell culture media was replenished daily. All experiments contained
604 appropriate vehicle controls (DMSO or sterile H_2O).

605 *RNA isolation and quantification*

606 For quantitative RT-PCR analysis and RNA-sequencing (RNA-seq), RNA was isolated
607 from *h*MPCs and using Omega E.Z.N.A.® Total RNA Kit I (Omega) according to the
608 manufacturer's instructions. RNA was isolated from skeletal muscle biopsy tissue using Trizol
609 Reagent (Ambion) as per manufacturer's instructions. RNA quantity was determined
610 spectrophotometrically.

611 *Quantitative RT-PCR*

612 Gene expression was measured using quantitative RT-PCR. cDNA was synthesized via
613 reverse transcription of extracted RNA using the Applied Biosystems High-Capacity cDNA
614 Reverse Transcription Kit. The Taqman Gene Expression System (Applied Biosystems) was
615 used to measure mRNA expression levels of phosphoglycerate dehydrogenase (*PHGDH*,
616 HS00358823), phosphoserine aminotransferase 1 (*PSAT1*, Hs00268565), and phosphoserine
617 phosphatase (*PSPH*, Hs01921296). All samples were normalized to *18S* (Hs99999901)
618 expression.

619 *RNA library preparation and sequencing*

620 Prior to RNA-seq, RNA quality was determined using an AATI Fragment Analyzer; all
621 samples had an RNA quality number >8.5. The NEBNext Ultra II RNA Library Prep Kit (New
622 England Biolabs) was used to generate TruSeq-barcoded RNA-Seq libraries. Libraries were
623 quantified with the Qubit 2.0 (dsDNA HS kit; Thermo Fisher) and size distribution was
624 measured with a Fragment Analyzer (Advanced Analytical) before pooling. A NextSeq500
625 (Illumina) was used for sequencing, and a minimum of 20 M single-end 75 bp reads per library
626 were obtained. Cutadapt v1.8 was used to trim low quality reads and adaptor sequences
627 (parameters: -m 50 -q 20 -a AGATCGGAAGAGCACACGTCTGAACTCCAG–match-read-
628 wild cards) (Martin, 2011). Tophat v2.1 was used to map reads to the reference genome

(parameters:-library-type=fr-firststrandon-no-novel-juncs-G<ref_genes.gtf>) (Kim et al., 2013). Differential gene expression analysis was performed using *edgeR* (McCarthy et al., 2012). Only genes with at least 2 counts per million in at least three of the samples were retained for analysis.

Immunoblot analysis

For immunoblot analysis, protein was isolated from *h*MPCs with RIPA buffer containing phosphatase (PhosSTOP, Roche) and protease (cOmplete, Roche) inhibitors. The protein concentration was quantified by BCA. 8-15 μg of protein was loaded on 10% SDS gels and transferred to PVDF membranes. Membranes were incubated in primary antibodies PHGDH (Proteintech), PSAT1 (Proteintech), PSPH (Proteintech), SHMT1 (Stover laboratory) (Woeller et al., 2007), SHMT2 (Stover laboratory) (Anderson and Stover, 2009), Cyclin D1 (Cell Signaling), ATF4 (Cell Signaling), phosphorylated (Ser51) p-EIF2α (Cell Signaling), and total EIF2α (Cell Signaling) diluted (1:1000) in a chemiluminescent blocking buffer (bl∅kTM – CH, Millipore) overnight at 4oC. After the overnight incubation, membranes were washed with 0.1% Tween in tris-buffered saline before incubation with appropriate secondary antibody (rabbit, Proteintech; goat, Thermo Scientific; mouse, Proteintech; goat, Piece) at a 1:100000 dilution in a chemiluminescent blocking buffer, at room temperature, for 60 min. Membranes were visualized after a brief incubation in SuperSignalTM West Femto (Thermo Scientific) on the Bio-Rad ChemiDoc MP. Protein expression was normalized to α-TUBULIN expression (Cell Signaling) using the ImageLab 4.1 software (Bio-Rad).

Live and dead cell counting

Live cell number was determined by co-staining cells with Hoechst 33342 (to identify number of nuclei, Life Technologies) and propidium iodide (to identify dead cells, ThermoFisher Scientific). The number of live cells was determined by subtracting the number of propidium

652 iodide positive cells from the Hoechst 33342 positive cells as identified using the Celigo imaging
653 cytometer (Nexcelcom).

654 *Cell cycle analysis*

655 For cell cycle analysis, *h*MPCs were pelleted, washed with ice-cold PBS, re-pelleted and
656 resuspended in PBS then fixed in 3:1 volume:volume 100% ice-cold ethanol before being stored
657 at 4 ^{o}C overnight. The following day, cells were pelleted, washed with ice-cold PBS, and
658 resuspended in 400 µL PBS containing 2 mM EDTA. Cell suspensions were incubated with 100
659 µL 10 mg/mL RNAse A (VWR) for 30 min at 37^{o}C, to degrade RNA, followed by DNA staining
660 with 50 µL of 1 mg/mL propidium iodide for 30 min, in the dark, at room temperature.
661 Propidium iodide intensity was measured using a flow cytometer (BD Aria Fusion). The
662 percentage of the total population of cells in G1, S-phase, G2 cells were determined using
663 FlowJo's (Becton, Dickinson, and Company) univariate platform.

664 *5-bromo-2'-deoxyuridine (BrdU) incorporation*

665 To determine the proportion of cells actively synthesizing DNA, *h*MPCs were pulsed
666 with BrdU for 24 hours. *h*MPCs were washed with prewarmed PBS before being fixed in ice-
667 cold methanol for 5 min. Cells were washed with PBS before 30 min of acid hydrolysis and cell-
668 permeabilization in 2 N HCl prepared in 0.1% PBS-Tween20. Cells were washed with PBS
669 before being blocked in 1% BSA/10% normal goat serum/0.3 M glycine/0.1% PBS-Tween20
670 followed by washing in PBS. Fixed and blocked *h*MPCs were incubated overnight at 4^{o}C with an
671 anti-BrdU antibody (1:400 dilution, Biolegend) followed by PBS washes and a 60 min
672 incubation with an Alexa-Fluor 488 conjugated anti-mouse secondary antibody (Invitrogen).
673 Finally, *h*MPCs were washed with PBS and incubated with Hoechst 33342 before visualization
674 and analysis using the Celigo imaging cytometer (Nexcelcom).

675 *Glucose uptake*

676 Glucose uptake was measured based on the detection of 2-deoxyglucose-6-phosphate
677 uptake by a commercially available luminescence-based kit (Glucose Uptake-Glo™ Assay,
678 Promega) on a SpectraMax M3 (Molecular Devices). Values were normalized to total cell count
679 obtained from a parallel plate.

680 *Stable-Isotope Labeling, Metabolite Extraction, and GC-MS Analysis*

681 For isotopic labeling experiments, cells were cultured in 10 mM [U-$^{13}C_6$]glucose
682 (Cambridge Isotope Laboratories, Inc.) containing either 1000 µM serine/glycine or no
683 serine/glycine for 48 h prior to extraction. A medium exchange was performed after 24 hours.
684 On the day of extraction, polar metabolites were extracted as previously described (Cordes and
685 Metallo, 2019).

686 The upper aqueous phase was derivatized using a Gerstel MPS with 15 µL of 2% (w/v)
687 methoxyamine hydrochloride (Thermo Scientific) in pyridine (incubated for 60 min at 45°C) and
688 followed by 15 µL MTBSTFA with 1% tert-butyldimethylchlorosilane (Regis Technologies)
689 (incubated for 30 min at 45°C). Polar derivatives were analyzed by GC-MS using a DB-35MS
690 column (30 m x 0.25 mm i.d. x 0.25 µm) installed in an Agilent 7890B GC interfaced with an
691 Agilent 5977B MS with an XTR EI source using the following temperature program: 100°C
692 initial, increase by 3.5°C/min to 255°C, increase by 15°C/min to 320°C and hold for 3 min.

693 *Glutathione measurements*

694 Total and oxidized (GSSG) glutathione were measured using a commercially available
695 luminescence-based kit (GSH-GSSG Glo™ Assay, Promega) on a SpectraMax M3 (Molecular
696 Devices). The reduced (GSH) to oxidized GSSG ratio was determined by multiplying the GSSG
697 reading by 2, to account for each mole of oxidized GSSG producing two moles of total

glutathione, subtracting that number from the total glutathione levels and finally, dividing this value by the total GSSG reading. Values were normalized to total cell count obtained from a parallel plate.

Reactive oxygen species detection

To determine the intracellular level of ROS, *h*MPCs were pelleted and resuspended in 1 mL pre-warmed PBS with CellROX Green Reagent (Invitrogen), a cell-permeable dye which fluoresces green and binds to DNA upon oxidation, at a final concentration of 5 µM. After a 30 min incubation at 37$_{o}$C, *h*MPCs were washed with PBS before being fixed in 2% paraformaldehyde for 10 min at room temperature. *h*MPCs were again washed with PBS before finally being resuspended in 300 µL 0.5 mM EDTA in PBS and analyzed via flow cytometry (BD Aria Fusion).

NAD/NADH measurements

The reduced NAD (NADH) to oxidized NAD (NAD^+) ratio was determined in *h*MPCs via a commercially available luminescence-based kit (NAD/NADH Glo™ Assay, Promega) following the manufacturer's instructions. Luminescence values were obtained with a SpectraMax M3 (Molecular Devices) and normalized to total cell count obtained from a parallel plate.

Protein synthesis

The SUnSET Method (Schmidt et al., 2009) was used to quantify the rate of puromycin incorporation to approximate protein synthesis (Henrich, 2016). *h*MPCs were treated with 0.5 µg/mL puromycin (Thermo Fisher) for 30 min and then immediately harvested in RIPA buffer and protein was isolated as described above. Immunoblotting was performed, as described, using a primary antibody specific for puromycin (Millipore) diluted 1:1000 in a chemiluminescent

721 blocking buffer overnight, prior to incubation in secondary antibody (mouse, Proteintech) diluted
722 1:100000. *h*MPCs were incubated in SuperSignal™ West Femto (Thermo Scientific) and imaged
723 on the Bio-Rad ChemiDoc MP. Puromycin expression was normalized to the total protein level
724 in each respective lane as determined by Coomassie staining and imaging on the Bio-Rad
725 ChemiDoc MP using the ImageLab 4.1 software (Bio-Rad).

726 *Statistics*

727 Statistical analyses were performed in R Studio (Version 1.0.136). For metabolite
728 analysis of whole skeletal muscle tissue, the normalcy of the distribution of each amino acid was
729 assessed by the Shapiro-Wilk test. If data were determined to be normally distributed, they were
730 compared via an unpaired t-test otherwise they were compared by a Mann-Whitney U-test. The
731 correlation between skeletal muscle serine levels and age were determine using a Pearson
732 correlation coefficient. When comparing gene and protein expression between age groups, an
733 unpaired t-test was performed. For cell counting experiments, two-way analysis of variance
734 (ANOVA) was performed with time and treatment being the main factors. A Tukey *post hoc* test
735 was performed if the interaction term was significant ($P<0.05$). For all *h*MPC assays, either a
736 paired t-test or a repeated measures ANOVA was employed.

737

738

739

740

741

742

743

Acknowledgments

This work was financially supported by a President's Council of Cornell Women Award (to A.T.M), Cornell University Division of Nutritional Sciences funds (to A.T.M), and a Canadian Institutes for Health Research Doctoral Foreign Study Award (to B.J.G), and NIH grant R01CA234245 (to C.M.M.).

Author Contributions

Conceptualization, B.J.G, P.J.S, and A.E.T..; Methodology, B.J.G, M.S.F., P.J.S., and A.E.T..; Investigation, B.J.G, J.E.B, M.E.G., E.W.L., and M.K.H.; Resources, E.B., P.J.S, M.S.F., B.D.C., C.M., and A.E.T.; Writing – Original Draft, B.J.G. and A.E.T.; Writing – Review and Editing, B.J.G., J.E.B, M.E.G., E.W.L., M.K.H., P.J.S., M.S.F., B.D.C., C.M.M., and A.E.T.; Supervision, A.E.T.

Declaration of Interests

The authors declare no conflicts of interest.

References

Anderson, D.D., and Stover, P.J. (2009). SHMT1 and SHMT2 are functionally redundant in nuclear de novo thymidylate biosynthesis. PLoS One *4*.

Bergström, J., Fürst, P., Norée, L.O., and Vinnars, E. (2017). Intracellular free amino acid concentration in human muscle tissue. J. Appl. Physiol. *36*, 693–697.

Blau, H.M., Cosgrove, B.D., and Ho, A.T.V. (2015). The central role of muscle stem cells in regenerative failure with aging. Nat. Med. *21*, 854–862.

Brack, A.S., Conboy, M.J., Roy, S., Lee, M., Kuo, C.J., Keller, C., and Rando, T.A. (2007). Increased Wnt signaling during aging alters muscle stem cell fate and increases fibrosis. Science (80-.). *317*, 807–810.

Caldow, M.K., Ham, D.J., Godeassi, D.P., Chee, A., Lynch, G.S., and Koopman, R. (2016). Glycine supplementation during calorie restriction accelerates fat loss and protects against further muscle loss in obese mice. Clin. Nutr. *35*, 1118–1126.

Carnwath, J.W., and Shotton, D.M. (1987). Muscular dystrophy in the mdx mouse: Histopathology of the soleus and extensor digitorum longus muscles. J. Neurol. Sci. *80*, 39–54.

Conboy, I.H., Conboy, M.J., Smythe, G.M., and Rando, T.A. (2003). Notch-Mediated Restoration of Regenerative Potential to Aged Muscle. Science (80-.). *302*, 1575–1577.

Conboy, I.M., Conboy, M.J., Wagers, A.J., Girma, E.R., Weissman, I.L., and Rando, T.A. (2005). Rejuvenation of aged progenitor cells by exposure to a young systemic environment. Nature *433*, 760–764.

Cordes, T., and Metallo, C.M. (2019). Quantifying intermediary metabolism and lipogenesis in cultured mammalian cells using stable isotope tracing and mass spectrometry. In Methods in Molecular Biology, pp. 219–241.

790 DeNicola, G.M., Chen, P.H., Mullarky, E., Sudderth, J.A., Hu, Z., Wu, D., Tang, H., Xie, Y.,
791 Asara, J.M., Huffman, K.E., et al. (2015). NRF2 regulates serine biosynthesis in non-small cell
792 lung cancer. Nat. Genet. *47*, 1475–1481.
793 Diehl, F.F., Lewis, C.A., Fiske, B.P., and Vander Heiden, M.G. (2019). Cellular redox state
794 constrains serine synthesis and nucleotide production to impact cell proliferation. Nat. Metab.
795 Dufresne, M.J.P., MacLeod, J., Rogers, J., and Sanwal, B.D. (1976). Serine auxotrophy of
796 myoblasts in primary and secondary culture. Biochem. Biophys. Res. Commun. *70*, 1085–1090.
797 Dunn, W.B., Lin, W., Broadhurst, D., Begley, P., Brown, M., Zelena, E., Vaughan, A.A.,
798 Halsall, A., Harding, N., Knowles, J.D., et al. (2014). Molecular phenotyping of a UK
799 population: defining the human serum metabolome. Metabolomics *11*, 9–26.
800 Egerman, M.A., Cadena, S.M., Gilbert, J.A., Meyer, A., Nelson, H.N., Swalley, S.E., Mallozzi,
801 C., Jacobi, C., Jennings, L.L., Clay, I., et al. (2015). GDF11 Increases with Age and Inhibits
802 Skeletal Muscle Regeneration. Cell Metab. *22*, 164–174.
803 Fazelzadeh, P., Hangelbroek, R.W.J., Tieland, M., De Groot, L.C.P.G.M., Verdijk, L.B., Van
804 Loon, L.J.C., Smilde, A.K., Alves, R.D.A.M., Vervoort, J., Müller, M., et al. (2016). The Muscle
805 Metabolome Differs between Healthy and Frail Older Adults. J. Proteome Res. *15*, 499–509.
806 Fulle, S., Di Donna, S., Puglielli, C., Pietrangelo, T., Beccafico, S., Bellomo, R., Protasi, F., and
807 Fanò, G. (2005). Age-dependent imbalance of the antioxidative system in human satellite cells.
808 Exp. Gerontol. *40*, 189–197.
809 Gallot, Y.S., Straughn, A.R., Bohnert, K.R., Xiong, G., Hindi, S.M., and Kumar, A. (2018).
810 MyD88 is required for satellite cell-mediated myofiber regeneration in dystrophin-deficient mdx
811 mice. Hum. Mol. Genet. *27*, 3449–3463.
812 Gannon, M.C., Nuttall, J.A., and Nuttall, F.Q. (2002). The metabolic response to ingested

glycine. Am. J. Clin. Nutr. *76*, 1302–1307.

Garofalo, K., Penno, A., Schmidt, B.P., Lee, H.J., Frosch, M.P., Von Eckardstein, A., Brown, R.H., Hornemann, T., and Eichler, F.S. (2011). Oral L-serine supplementation reduces production of neurotoxic deoxysphingolipids in mice and humans with hereditary sensory autonomic neuropathy type 1. J. Clin. Invest. *121*, 4735–4745.

Gheller, B.J., Blum, J.E., Merritt, E.K., Cummings, B.P., and Thalacker-Mercer, A.E. (2019a). Peptide YY (PYY) is expressed in human skeletal muscle tissue and expanding human muscle progenitor cells. Front. Physiol. *10*.

Gheller, B.J., Blum, J., Soueid-Baumgarten, S., Bender, E., Cosgrove, B.D., and Thalacker-Mercer, A. (2019b). Isolation, Culture, Characterization, and Differentiation of Human Muscle Progenitor Cells from the Skeletal Muscle Biopsy Procedure. J. Vis. Exp.

Ham, D.J., Murphy, K.T., Chee, A., Lynch, G.S., and Koopman, R. (2014). Glycine administration attenuates skeletal muscle wasting in a mouse model of cancer cachexia. Clin. Nutr. *33*, 448–458.

Ham, D.J., Caldow, M.K., Chhen, V., Chee, A., Wang, X., Proud, C.G., Lynch, G.S., and Koopman, R. (2016). Glycine restores the anabolic response to leucine in a mouse model of acute inflammation. Am. J. Physiol. - Endocrinol. Metab. *310*, E970–E981.

Ham, D.J., Gardner, A., Kennedy, T.L., Trieu, J., Naim, T., Chee, A., Alves, F.M., Caldow, M.K., Lynch, G.S., and Koopman, R. (2019). Glycine administration attenuates progression of dystrophic pathology in prednisolone-treated dystrophin/utrophin null mice. Sci. Rep. *9*, 12982.

Hamanaka, R.B., Bennett, B.S., Cullinan, S.B., and Diehl, J.A. (2005). PERK and GCN2 contribute to eIF2α phosphorylation and cell cycle arrest after activation of the unfolded protein response pathway. Mol. Biol. Cell *16*, 5493–5501.

836 Harding, H.P., Zhang, Y., Zeng, H., Novoa, I., Lu, P.D., Calfon, M., Sadri, N., Yun, C., Popko,
837 B., Paules, R., et al. (2003). An integrated stress response regulates amino acid metabolism and
838 resistance to oxidative stress. Mol. Cell *11*, 619–633.
839 Henrich, C.J. (2016). A microplate-based nonradioactive protein synthesis assay: Application to
840 TRAIL sensitization by protein synthesis inhibitors. PLoS One.
841 Holcik, M., and Sonenberg, N. (2005). Translational control in stress and apoptosis. Nat. Rev.
842 Mol. Cell Biol. *6*, 318–327.
843 Hosios, A.M., Hecht, V.C., Danai, L. V., Johnson, M.O., Rathmell, J.C., Steinhauser, M.L.,
844 Manalis, S.R., and Vander Heiden, M.G. (2016). Amino Acids Rather than Glucose Account for
845 the Majority of Cell Mass in Proliferating Mammalian Cells. Dev. Cell.
846 Houtkooper, R.H., Argmann, C., Houten, S.M., Canto, C., Jeninga, E.H., Andreux, Pelope A.,
847 Thomas, C., Doenlen, R., Schoonjans, K., and Auwerx, J. (2011). The metabolic footprint of
848 aging in mice. Sci. Rep. *1*.
849 Katsanos, C.S., Kobayashi, H., Sheffield-Moore, M., Aarsland, A., and Wolfe, R.R. (2006). A
850 high proportion of leucine is required for optimal stimulation of the rate of muscle protein
851 synthesis by essential amino acids in the elderly. Am. J. Physiol. - Endocrinol. Metab. *291*.
852 Kawase, A., Ito, A., Yamada, A., and Iwaki, M. (2015). Age-related changes in mRNA levels of
853 hepatic transporters, cytochrome P450 and UDP-glucuronosyltransferase in female rats. Eur. J.
854 Drug Metab. Pharmacokinet. *40*, 239–244.
855 Kim, D., Pertea, G., Trapnell, C., Pimentel, H., Kelley, R., and Salzberg, S.L. (2013). TopHat2:
856 Accurate alignment of transcriptomes in the presence of insertions, deletions and gene fusions.
857 Genome Biol. *14*.
858 Kitzmann, M., Carnac, G., Vandromme, M., Primig, M., Lamb, N.J.C., and Fernandez, A.

(1998). The muscle regulatory factors MyoD and Myf-5 undergo distinct cell cycle-specific expression in muscle cells. J. Cell Biol.

Koopman, R., Caldow, M.K., Ham, D.J., and Lynch, G.S. (2017). Glycine metabolism in skeletal muscle: Implications for metabolic homeostasis. Curr. Opin. Clin. Nutr. Metab. Care *20*, 237–242.

Kouchiwa, T., Wada, K., Uchiyama, M., Kasezawa, N., Niisato, M., Murakami, H., Fukuyama, K., and Yokogoshi, H. (2012). Age-related changes in serum amino acids concentrations in healthy individuals. Clin. Chem. Lab. Med. *50*, 861–870.

L'Honoré, A., Commère, P.H., Negroni, E., Pallafacchina, G., Friguet, B., Drouin, J., Buckingham, M., and Montarras, D. (2018). The role of Pitx2 and Pitx3 in muscle 1 stem cells gives new insights into P38α MAP kinase and redox regulation of muscle regeneration. Elife *7*.

Labuschagne, C.F., van den Broek, N.J.F., Mackay, G.M., Vousden, K.H., and Maddocks, O.D.K. (2014). Serine, but not glycine, supports one-carbon metabolism and proliferation of cancer cells. Cell Rep. *7*, 1248–1258.

Ma, E.H., Bantug, G., Griss, T., Condotta, S., Johnson, R.M., Samborska, B., Mainolfi, N., Suri, V., Guak, H., Balmer, M.L., et al. (2017). Serine Is an Essential Metabolite for Effector T Cell Expansion. Cell Metab. *25*, 345–357.

Martin, M. (2011). Cutadapt removes adapter sequences from high-throughput sequencing reads. EMBnet.Journal *17*, 10.

McCarthy, D.J., Chen, Y., and Smyth, G.K. (2012). Differential expression analysis of multifactor RNA-Seq experiments with respect to biological variation. Nucleic Acids Res. *40*, 4288–4297.

Menni, C., Kastenmüller, G., Petersen, A.K., Bell, J.T., Psatha, M., Tsai, P.C., Gieger, C.,

882 Schulz, H., Erte, I., John, S., et al. (2013). Metabolomic markers reveal novel pathways of ageing
883 and early development in human populations. Int. J. Epidemiol. *42*, 1111–1119.
884 Minet, A.D., and Gaster, M. (2012). Cultured senescent myoblasts derived from human vastus
885 lateralis exhibit normal mitochondrial ATP synthesis capacities with correlating concomitant
886 ROS production while whole cell ATP production is decreased. Biogerontology *13*, 277–285.
887 Mitchell, W.K., Phillips, B.E., Williams, J.P., Rankin, D., Lund, J.N., Wilkinson, D.J., Smith, K.,
888 and Atherton, P.J. (2015). The impact of delivery profile of essential amino acids upon skeletal
889 muscle protein synthesis in older men: Clinical efficacy of pulse vs. bolus supply. Am. J.
890 Physiol. - Endocrinol. Metab. *309*, E450–E457.
891 Pavlidou, T., Rosina, M., Fuoco, C., Gerini, G., Gargioli, C., Castagnoli, L., and Cesareni, G.
892 (2017). Regulation of myoblast differentiation by metabolic perturbations induced by metformin.
893 PLoS One *12*.
894 Polymenis, M., and Aramayo, R. (2015). Translate to divide: control of the cell cycle by protein
895 synthesis. Microb. Cell *2*, 94–104.
896 Riddle, E.S., Bender, E.L., and Thalacker-Mercer, A.E. (2018a). Expansion capacity of human
897 muscle progenitor cells differs by age, sex, and metabolic fuel preference. Am. J. Physiol. - Cell
898 Physiol. *315*, C643–C652.
899 Riddle, E.S., Bender, E.L., and Thalacker-Mercer, A. (2018b). Transcript profile distinguishes
900 variability in human myogenic progenitor cell expansion capacity. Physiol. Genomics.
901 Rodgers, J.T., King, K.Y., Brett, J.O., Cromie, M.J., Charville, G.W., Maguire, K.K., Brunson,
902 C., Mastey, N., Liu, L., Tsai, C.-R., et al. (2014). mTORC1 controls the adaptive transition of
903 quiescent stem cells from G0 to G(Alert). Nature *509*, 393–396.
904 Schmidt, E.K., Clavarino, G., Ceppi, M., and Pierre, P. (2009). SUnSET, a nonradioactive

905 method to monitor protein synthesis. Nat. Methods *6*, 275–277.

906 Seale, P., Sabourin, L.A., Girgis-Gabardo, A., Mansouri, A., Gruss, P., and Rudnicki, M.A.

907 (2000). Pax7 is required for the specification of myogenic satellite cells. Cell.

908 Sekhar, R. V., Patel, S.G., Guthikonda, A.P., Reid, M., Balasubramanyam, A., Taffet, G.E., and

909 Jahoor, F. (2011). Deficient synthesis of glutathione underlies oxidative stress in aging and can

910 be corrected by dietary cysteine and glycine supplementation. Am. J. Clin. Nutr. *94*, 847–853.

911 Sidrauski, C., McGeachy, A.M., Ingolia, N.T., and Walter, P. (2015). The small molecule ISRIB

912 reverses the effects of eIF2α phosphorylation on translation and stress granule assembly. Elife

913 *2015*.

914 Sinha, M., Jang, Y.C., Oh, J., Khong, D., Wu, E.Y., Manohar, R., Miller, C., Regalado, S.G.,

915 Loffredo, F.S., Pancoast, J.R., et al. (2014). Restoring systemic GDF11 levels reverses age-

916 related dysfunction in mouse skeletal muscle. Science (80-.).

917 Sousa-Victor, P., Gutarra, S., García-Prat, L., Rodriguez-Ubreva, J., Ortet, L., Ruiz-Bonilla, V.,

918 Jardí, M., Ballestar, E., González, S., Serrano, A.L., et al. (2014). Geriatric muscle stem cells

919 switch reversible quiescence into senescence. Nature *506*, 316–321.

920 Sun, K., Wu, Z., Ji, Y., and Wu, G. (2016). Glycine Regulates Protein Turnover by Activating

921 Protein Kinase B/Mammalian Target of Rapamycin and by Inhibiting MuRF1 and Atrogin-1

922 Gene Expression in C2C12 Myoblasts. J. Nutr. *146*, 2461–2467.

923 Wallace, M., Green, C.R., Roberts, L.S., Lee, Y.M., McCarville, J.L., Sanchez-Gurmaches, J.,

924 Meurs, N., Gengatharan, J.M., Hover, J.D., Phillips, S.A., et al. (2018). Enzyme promiscuity

925 drives branched-chain fatty acid synthesis in adipose tissues. Nat. Chem. Biol. *14*, 1021–1031.

926 Woeller, C.F., Anderson, D.D., Szebenyi, D.M.E., and Stover, P.J. (2007). Evidence for small

927 ubiquitin-like modifier-dependent nuclear import of the thymidylate biosynthesis pathway. J.

928 Biol. Chem. *282*, 17623–17631.

929 Xu, X., Wilschut, K.J., Kouklis, G., Tian, H., Hesse, R., Garland, C., Sbitany, H., Hansen, S.,

930 Seth, R., Knott, P.D., et al. (2015). Human Satellite Cell Transplantation and Regeneration from

931 Diverse Skeletal Muscles. Stem Cell Reports *5*, 419–434.

932 Zismanov, V., Chichkov, V., Colangelo, V., Jamet, S., Wang, S., Syme, A., Koromilas, A.E., and

933 Crist, C. (2016). Phosphorylation of eIF2α is a Translational Control Mechanism Regulating

934 Muscle Stem Cell Quiescence and Self-Renewal. Cell Stem Cell *18*, 79–90.

935

936

937

938

939

940

941

942

943

944

945

946

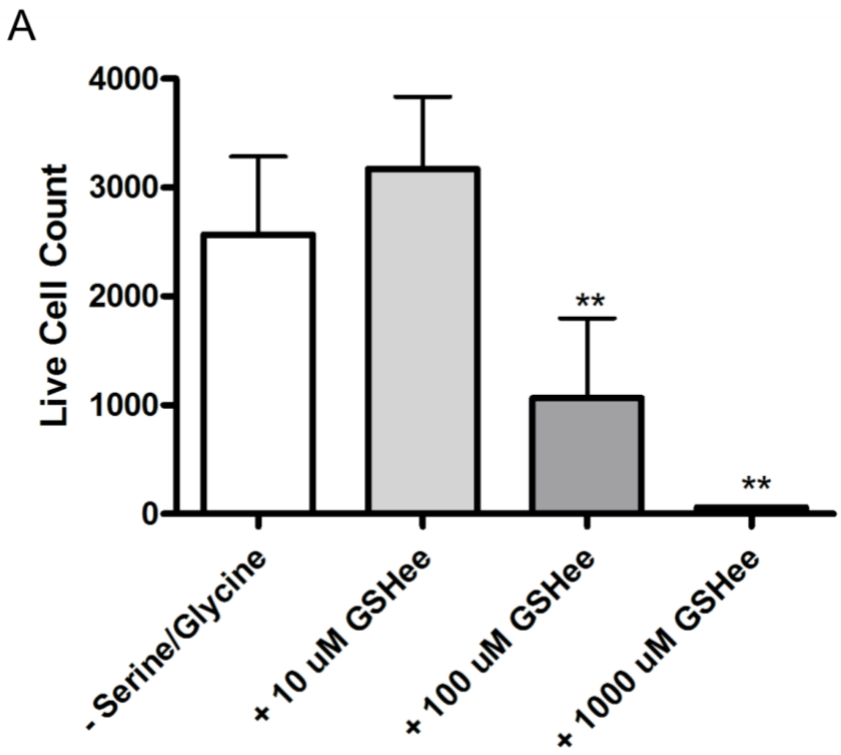

947

948 **Figure S1.** Glutathione ethyl ester is toxic to *h*MPCs at high doses

949

950 A) Live cell count after 5 days of GSHee (glutathione ethyl ester) supplementation in

951 serine/glycine restricted media.

952 All experiments were repeated with *h*MPCs derived from the same 5 donors. **P<0.01 relative

953 to serine/glycine restricted control. Data are expressed as mean ± SD.

954

955

956

957

958

959

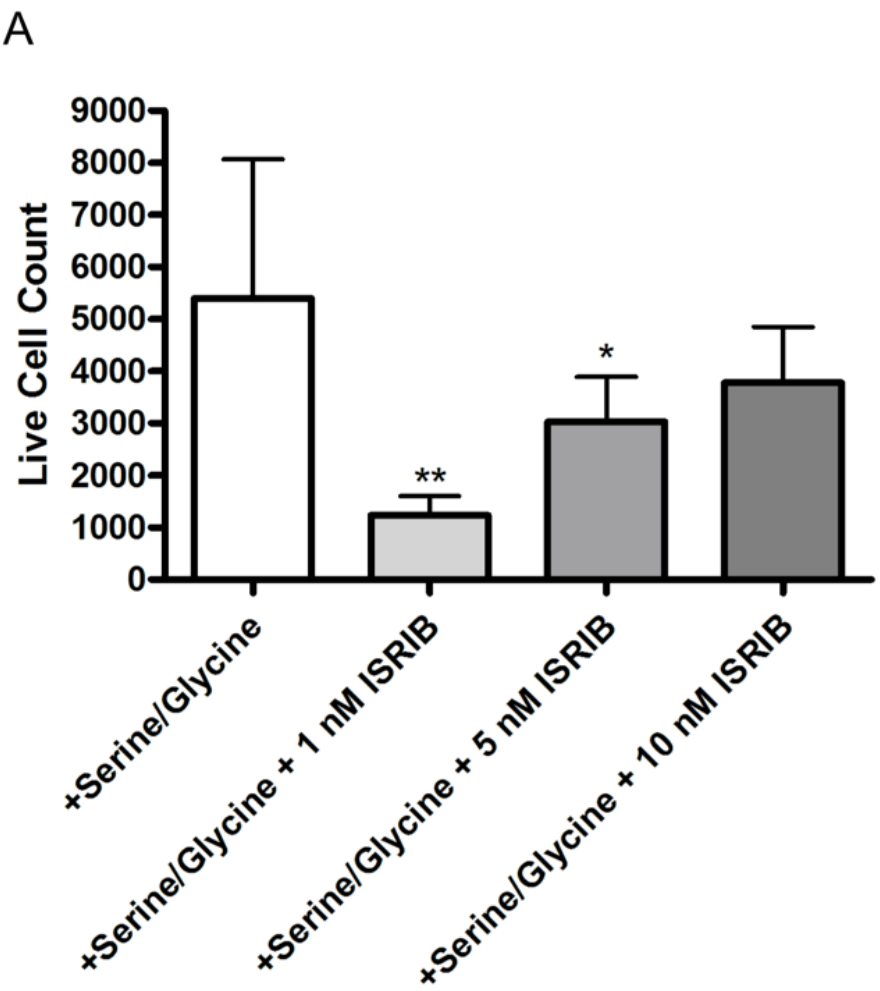

960

961

962

963 **Figure S2.** ISRIB reduces *h*MPC number in the presence of serine/glycine

964

965 A) Live cell count after 5 days of ISRIB supplementation in serine/glycine replete media.

966 All experiments were repeated with *h*MPCs derived from the same 5 donors. **P<0.01,

967 **P<0.01 relative to serine/glycine replete control. Data are expressed as mean ± SD.

968

969

Supplementary Tables

Supplementary Table 1. List of Differentially Expressed Genes in *h*MPCs Cultured in Serine/Glycine Replete and Serine/Glycine Restricted Media